GEOPHYSICAL RESEARCH LETTERS, VOL. 37, L11602, doi:10.1029/2010GL043556, 2010

Role of vertical migration in biogenic ocean mixing

John O. Dabiri[1]

Received 7 April 2010; revised 30 April 2010; accepted 3 May 2010; published 8 June 2010.

[1] Recent efforts to empirically measure and numerically simulate biogenic ocean mixing have consistently observed low mixing efficiency. This suggests that the buoyancy flux achieved by swimming animals in the ocean may be negligible in spite of the observed large kinetic energy dissipation rates. The present letter suggests that vertical migration across isopycnals may be necessary in order to generate overturning and subsequent mixing at length scales significantly larger than the individual animals. The animal-fluid interactions are simulated here using a simplified potential flow model of solid spheres migrating vertically in a stably stratified fluid. The interaction of successive solid bodies with each parcel of fluid is shown to lead, under certain conditions, to vertical displacement of the fluid parcels over distances much larger than the individual body size. These regions of displaced fluid are unstably stratified and, hence, amenable to large-scale overturning and efficient mixing. **Citation:** Dabiri, J. O. (2010), Role of vertical migration in biogenic ocean mixing, *Geophys. Res. Lett.*, *37*, L11602, doi:10.1029/2010GL043556.

1. Introduction

[2] The proposition that swimming animals can influence large-scale ocean mixing and circulation was introduced in jest by *Munk* [1966, also personal communication, 2007], but has received more serious attention in recent years [*Huntley and Zhou*, 2004; *Dewar et al.*, 2006]. *Kunze et al.* [2006] observed significantly elevated kinetic energy dissipation rates in the vicinity of aggregations of krill, and subsequently noted shear fluctuations at length scales up to one meter, significantly larger than the individual animals [*Kunze et al.*, 2007]. By contrast, recent field measurements by *Gregg and Horne* [2009] and *Lorke and Probst* [2010] and numerical simulations by J.-L. Thiffeault and S. Childress (Stirring by swimming bodies, arXiv:0911.5511v1, 2010) all indicate negligible buoyancy flux due to animal swimming. These studies observe that the displacement of fluid across isopycnals occurs at length scales that are small relative to typical oceanic values of the Ozmidov buoyancy length scale, which measures the vertical size of the largest overturning eddies in a stratified fluid [*Thorpe*, 2005]. As noted by *Visser* [2007], fluid motion at such small scales is primarily dissipated by the fluid viscosity and therefore cannot contribute to large-scale diapycnal mixing.

[3] A notable difference between the measurements of *Kunze et al.* [2006] and subsequent investigations is that the former experiments were carried out on plankton during vertical migration. By contrast, the field measurements of schooling fish by *Gregg and Horne* [2009] and *Lorke and Probst* [2010] and the numerical simulations by Thiffeault and Childress (arXiv:0911.5511v1, 2010) are missing this behavioral component of animal swimming. The vertical motion of the entire aggregation potentially introduces new physics to the fluid mixing problem, as the composite interaction of the animals with a given parcel of fluid is no longer isotropic. Instead, a statistical bias in the vertical direction and, importantly, across isopcynals, is introduced. This letter investigates the effect of vertical migration on the diapycnal stirring that is achieved.

[4] The numeral model utilized in this study treats the swimming animals as rigid spherical bodies in a potential flow. This simplification allows the model to serve as a lower-bound estimate on the mixing, for at least two reasons. First, *Katija and Dabiri* [2009] demonstrated that viscosity in the fluid substantially enhances the fluid displacement that occurs as an animal swims through fluid; that benefit is not present in the current model. Second, vortex shedding from solid bodies in an aggregation has been observed to substantially enhance the volume of fluid that remains trapped and carried with the aggregation [*White and Nepf*, 2003]; that effect is also missing from the current model. Nonetheless, the simplified potential flow model will be shown sufficient to achieve fluid displacement over length scales much larger than the individual bodies. Given this result, it is expected that the phenomena in the real ocean, with viscosity and vortex shedding present, will be even more pronounced.

[5] Finally, it is useful to note that although the spheres in this potential flow model are not strictly self-propelled like a real animal, they do exhibit a momentum-less wake that is consistent with the fluid dynamic signature of a steadily-swimming, self-propelled animal [*Lighthill*, 1975]. This is a unique benefit of modeling rigid bodies in potential flow as opposed to finite Reynolds number flow.

[6] To be sure, the simulation of rigid spheres in unbounded potential flow neglects two physical processes that might initially appear to mitigate the stirring of the water column by swimming animals. First, an animal swimming forward in viscous fluid must create a rearward momentum flux in order to overcome hydrodynamic drag. This flux of momentum results in a corresponding mass flux in the direction opposite to the migration. Second, fluid mass conservation requires that forward advection of fluid in the vicinity of the migrating animal must be compensated by a rearward mass flux elsewhere in the flow. However, as long as the forward and rearward transport processes are spatially distinct, both processes contribute to stirring rather than counteracting one another. Indeed, the dispersion coefficient used to quantify fluid mixing depends on the mean squared displacement of fluid particles, and not on the sign (i.e., forward or rearward direction) of the displacement [*Batchelor and Townsend*, 1956; *Eames and Bush*, 1999]. Therefore, a

[1]Graduate Aeronautical Laboratories and Bioengineering, California Institute of Technology, Pasadena, California, USA.

0094-8276/10/2010GL043556

distinction between forward and rearward advection processes is unnecessary for the present mixing problem. The absence of significant rearward advection in the flow of the rigid spheres studied presently lends additional support to the notion that the problem considered here is a lower-bound estimate for the biogenic mixing process, since rearward fluxes make no significant contribution to the mean squared fluid displacements observed in unbounded potential flow.

2. Methods

[7] Let us consider the advection of a horizontal patch of fluid of width D in a stratified fluid with buoyancy frequency $N = \sqrt{\frac{-g}{\rho}\frac{d\rho}{dz}}$, where g is gravitational acceleration, ρ is the nominal fluid density, and z is the depth coordinate. In the ocean, the buoyancy frequency is typically between 10^{-4} and 10^{-2} s^{-1} [*Wunsch and Ferrari*, 2004]. The motion of the fluid patch is induced by the vertical passage of an array of spheres (nominally 1-cm diameter and neutrally buoyant) migrating at speed U equal to one body diameter per second in a single vertical plane. The spheres are assumed to be well-spaced such that the fluid patch is influenced by a single sphere at any time. This assumption is in the spirit of the model of Thiffeault and Childress (arXiv:0911.5511v1, 2010), and is also consistent with a lower-bound estimate of biogenic mixing since transport will be further enhanced for more closely spaced bodies [*White and Nepf*, 2003]. The velocity field of each sphere of diameter D has components [*Turner*, 1964]

$$u_r = \frac{dr}{dt} = -\left(1 - \frac{D^3}{8r^3}\right)\cos\theta \tag{1}$$

$$u_\theta = r\frac{d\theta}{dt} = \left(1 + \frac{D^3}{16r^3}\right)\sin\theta \tag{2}$$

where r is the radial coordinate and θ is the angular coordinate measured from the direction of oncoming flow (in the reference frame of the migrating sphere). By evaluation of equations (1) and (2) in the reference frame of the sphere, it is straightforward to show that the net advection of fluid particles surrounding the sphere is in the same direction as the sphere motion [cf. *Eames and Hunt*, 1997; *Eames and Bush*, 1999].

[8] Since the fluid stratification is in the regime $ND/U \ll 1$, its effect on fluid advection can be modeled by an effective velocity, given by dimensional analysis as

$$u_b = -\sqrt{\frac{-g}{\rho}\frac{d\rho}{dz}}(z - z_0)\hat{\mathbf{k}} \tag{3}$$

where z_0 is the density equilibrium depth of the fluid patch and $\hat{\mathbf{k}}$ is a unit vector in the vertical direction.

[9] The time-dependent Lagrangian trajectory $\mathbf{x}(t)$ of each fluid particle is given by integration of the evolution equation

$$\frac{d\mathbf{x}}{dt} = \mathbf{u}(r, \theta, z) \tag{4}$$

where $\mathbf{u}$ is the velocity field given by the sum of the components in equations (1)–(3), and the coordinate system (r, θ, z) is measured with respect to the instantaneous center of the sphere currently interacting with the tracked fluid patch. It is prudent to note that the velocity field given by the sum of equations (1)–(3) is no longer an exact solution of the potential flow equations, and this model for fluid stratification does not allow for the baroclinic formation of vorticity in the wake of each body (e.g., horseshoe vortices [*Eames and Hunt*, 1997]). The experiments of *White and Nepf* [2003] indicate that this vortex formation could further enhance the fluid transport studied presently; again, the absence of this phenomenon in the model is consistent with a lower-bound estimate of mixing.

[10] Equation (4) was solved using a forward Euler scheme with a time step $\Delta t = 0.005D/U$. Convergence of the simulations was verified by simulating the re-stratification of a vertically displaced horizontal row of fluid particles at buoyancy frequencies spanning the range $10^{-4} < N < 1$. For the mixing studies, a row of 20 equally spaced fluid particles spanning the fluid patch width D were initialized at their density equilibrium depth in the fluid. Each sphere was initialized one diameter below the patch and migrated vertically for four body diameters of travel before being removed from the domain and replaced by a new sphere below the patch at a horizontal position determined by the array configuration (e.g., at the same horizontal position for an inline array of bodies, or shifted horizontally for staggered arrays). Since in potential flow the effect of each body decays as r^{-3}, the effect of each body on patch advection is short-range, and the duration of influence is typically much less than the four diameters of travel simulated presently [*Eames and Bush*, 1999; Thiffeault and Childress, arXiv:0911.5511v1, 2010]. The instantaneous vertical displacement of the centroid of the tracked fluid patch was computed in each case. The fluid particle at the geometric center of the fluid patch was not included in the centroid calculation since, in many of the simulations described below, its position is coincident with the forward stagnation point of the migrating sphere and it is therefore advected infinitely far in principle [*Turner*, 1964].

[11] Several array configurations were tested at $N = 0$ s^{-1} (i.e., no stratification) and $N = 10^{-3}$ s^{-1} (i.e., intermediate ocean stratification); the results of four representative cases will be described in the following section. These are (a) single body vertical migration; (b) vertically-aligned array migration; (c) vertically-staggered array migration in two columns separated horizontally by $D/2$; and (d) vertically-staggered array migration in three columns separated horizontally by $D/2$. These configurations are illustrated in Figure 1.

3. Results

[12] Figure 2 plots the vertical displacement of the patch centroid for the four selected migration array patterns. The oscillations of each curve are due to the fore-aft looping of the particles as each solid body passes through the patch [*Darwin*, 1953]. The initial oscillation in Figure 2 is slightly shifted for the two-column staggered array relative to the others because the first body to pass through the patch is offset from the center of the patch. By contrast, in the single body, inline, and three-column cases, the first body passed through the center of the patch. This subtlety of the curves does not affect the longer-term patch advection.

[13] In the single body case, the net forward displacement of the patch centroid remains less than one body diameter. This is because, although the patch has the same width as the body diameter, fluid particles at the edge of the patch are

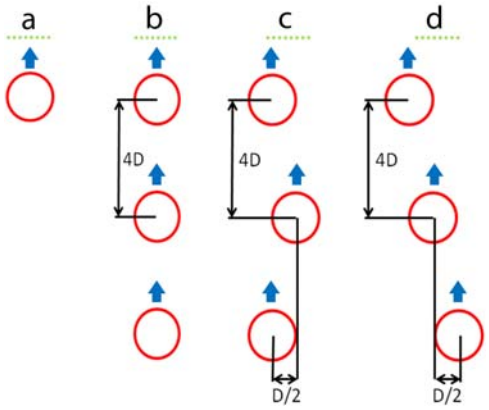

Figure 1. Vertical migration patterns. Tracked fluid patch indicated by dotted horizontal line. Direction of body migration indicated by blue arrows. (a) single body migration; (b) inline migration; (c) two-column staggered migration; (d) three-column staggered migration.

minimally advected by the sphere (see Animation S1 provided in the auxiliary material).[1] The maximum fluid displacement is achieved after less than four body diameters of travel, supporting the array construction methodology described in the previous section.

[14] The inline array demonstrates that the passage of successive bodies past the patch can lead to additional vertical displacement over time. As time progresses and particles are displaced further from their density equilibrium depth, the effect of re-stratification becomes evident. However, it is important to note that stratification in this range of buoyancy frequencies does not significantly impede the fluid displacement until after vertical displacement has begun to stagnate (see Animation S2 provided in the auxiliary material).

[15] Vertical displacement of the fluid patch is further enhanced if the bodies are staggered horizontally. In the two-column configuration, the edges of the patch are more effectively transported by the passing bodies than in the inline configuration. This result is intuitive given that the r^{-3} decay of the velocity field of each body is now alternately applied to the left- and right-hand sides of the patch (albeit at longer distance) instead of continuously applied to both sides, as was the case for the single body and inline cases (see Animation S3 provided in the auxiliary material).

[16] The vertical displacement of the patch can be further enhanced by staggering the vertically migrating bodies in three columns instead of two. In this way, the patch is efficiently displaced and continues its vertical advection for the duration of the simulation, over 300 body diameters of travel. Even in the case of the stratified fluid, displaced fluid length scales an order of magnitude greater than the individual body size are achieved (see Animation S4 provided in the auxiliary material).

4. Discussion

[17] The present letter has utilized a simplified model of animal-fluid interactions to demonstrate the role of vertical migration of aggregations in the transport of fluid across isopycnals. It is observed that overturning length scales substantially larger than the individual animals can be achieved due to vertical motion of the entire aggregation. While stable density stratification reduces the fluid displacement relative to a non-stratified fluid, it does not significantly impede the diapycnal stirring.

[18] Given the simplified nature of the present model, it is useful to consider the effect that more realistic physics would have on these results. While it is expected that the neglected fluid mechanics will further enhance the present results, a more quantitative analysis can make this claim more compelling.

[19] First, let us consider the effect of vortex shedding. In studies of fluid transport by arrays of vortex-shedding solid bodies, *White and Nepf* [2003] observed that the shed vortices tended to trap fluid near the solid bodies and thereby carry the fluid with the bodies. The vortex shedding was parameterized using the Strouhal number, $\mathrm{St} = FA/U$, where F is the frequency of vortex shedding, A is the vortex wake width, and U is the velocity of flow past the array of solid bodies. *White and Nepf* [2003] derived a corresponding longitudinal dispersion coefficient

$$D_v = \beta\kappa \mathrm{St}^{-1} U D^2 S^{-1} \tag{5}$$

where β and κ are empirical constants of proportionality ($\approx$1) that exhibit dependence on Reynolds number, body density and packing configuration; and S is the mean body spacing. Across a wide range of swimming animals, the Strouhal number lies in the range $0.2 < \mathrm{St} < 0.4$ [*Taylor et al.*, 2003].

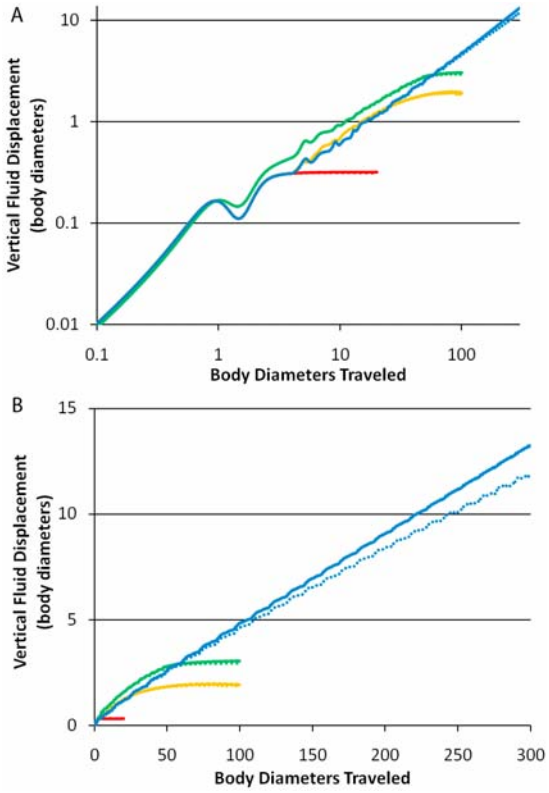

Figure 2. Vertical displacement of fluid patch centroid versus body diameters traveled. Red, single body; orange, inline migration; green, two-column staggered migration; blue, three-column staggered migration. Solid lines, $N = 0\ \mathrm{s}^{-1}$; dotted lines, $N = 10^{-3}\ \mathrm{s}^{-1}$; (a) log-log plot and (b) linear plot.

[1] Auxiliary materials are available in the HTML. doi:10.1029/2010GL043556.

Mindful of the caveat that swimming animals create thrust-producing wakes whereas *White and Nepf* [2003] studied drag-producing wakes, we may estimate the longitudinal dispersion due to vortex trapping in the animal wakes to be approximately $D_v \approx UD^2S^{-1}$. For example, plankton with characteristic body size of 10^{-2} m, vertical migration speed of 10^{-2} m s^{-1} and mean spacing of 10^{-2} m have an estimated longitudinal (i.e., diapycnal) dispersion $D_v \approx 10^{-4}$ m^2 s^{-1} due to vortex shedding alone. This dispersion is three orders of magnitude greater than molecular diffusion of heat in the ocean, and five orders of magnitude greater than molecular diffusion of salt [*Wunsch and Ferrari*, 2004].

[20] Viscosity in the fluid can enhance fluid displacement by migrating bodies, independently of vortex shedding. At a Reynolds numbers of 100 (e.g., a 1-cm plankton migrating at 1 cm s^{-1}), *Katija and Dabiri* [2009] found that the volume of fluid transported with moving solid bodies can be more than twice the fluid transported in the absence of viscosity. Since that volume of fluid is aligned and elongated in the direction of animal swimming, this increased volume of transported fluid increases the diapycnal fluid exchange. To confirm this result, simulations similar to those described presently were conducted in the limit of Stokes flow (J. O. Dabiri, unpublished material, 2009). In that case, even a single body was found to vertically displace the fluid patch over a distance nearly an order of magnitude greater than the individual body size.

[21] The calculations in this letter are based on the motion of a single fluid patch of width equal to the body diameter. However, the conditions under which substantial vertical transport is achieved correspond to situations in which the total horizontal area affected by the bodies is larger than the patch width (e.g., the three-column array). It is important to note that this is not an inconsistency in the model, nor does it bias the results by enhancing the vertical transport in a manner that is unphysical. Since only one body is permitted to interact with the patch at a time, one could extrapolate the present results to an infinitely-long horizontal row of particles by applying periodic boundary conditions at the lateral margins of the patterns in Figures 1c and 1d. The bodies will remain non-overlapping for the configurations studied in this letter, confirming the physical consistency of the model.

[22] The maximum duration of vertical migration simulated presently is 300 body diameters. Although the simulation of significantly longer migrations was beyond the scope of this study, it is expected that the curves corresponding to stratified fluid in Figure 2 will eventually turn over and return to zero ordinate values on a time scale dictated by the strength of the fluid stratification. The peak vertical displacement of each curve indicates the maximum overturning length scale that can be achieved. It appears that the single body, inline, and two-column arrays reach maximum vertical fluid displacement within the time frame of the simulations. The three-column array maintains its upward trajectory throughout, making it difficult to estimate the maximum overturning length scale. For the purposes of the present discussion, however, it suffices to note that order-of-magnitude increases in length scale are achieved, even in the stratified fluid.

[23] Returning to the original premise of this note, let us review the current evidence in support of biogenic mixing as a feasible large-scale ocean mixing mechanism. First, *Dewar et al.* [2006] provide an estimate of the global power input to biogenic mixing and show that it is comparable with the power inputs to physical oceanographic mixing processes like wind and tidal forcing. The present results suggest that an important next step is to further segregate this global estimate according to the contributions of vertically-migrating and non-migrating animals, since the former group can achieve significantly more efficient diapycnal mixing than the latter. The longitudinal dispersion model of *White and Nepf* [2003], when modified for vertically-migrating animals, suggests diapycnal diffusivity comparable with mean values in the ocean and several orders of magnitude greater than molecular diffusivities. Finally, the present note suggests a physical mechanism that can generate overturning length scales commensurate with large-scale mixing and high mixing efficiency.

[24] It remains to directly observe these biogenic mixing processes in the field or in direct numerical simulations. In either case, the primary point to be conveyed by this note is that future investigations may find it essential to capture the vertical migration of aggregations in order to successfully observe biogenic mixing.

[25] **Acknowledgments.** The author gratefully acknowledges support from the National Science Foundation programs in Biological Oceanography, Ocean Technology, Fluid Dynamics, and Energy for Sustainability.

References

Batchelor, G. K., and A. A. Townsend (1956), Turbulent diffusion, in *Surveys in Mechanics*, pp. 352–399, Cambridge Univ. Press, Cambridge, U. K.

Darwin, C. (1953), Note on hydrodynamics, *Proc. Cambridge Philos. Soc.*, *49*, 342–354, doi:10.1017/S0305004100028449.

Dewar, W. K., R. J. Bingham, R. L. Iverson, D. P. Nowacek, L. C. St. Laurent, and P. H. Wiebe (2006), Does the marine biosphere mix the ocean?, *J. Mar. Res.*, *64*, 541–561, doi:10.1357/002224006778715720.

Eames, I., and J. W. M. Bush (1999), Longitudinal dispersion of bodies fixed in a potential flow, *Proc. R. Soc. London A*, *455*, 3665–3686, doi:10.1098/rspa.1999.0471.

Eames, I., and J. C. R. Hunt (1997), Inviscid flow around bodies moving in a weak density gradient in the absence of buoyancy effects, *J. Fluid Mech.*, *353*, 331–355, doi:10.1017/S002211209700760X.

Gregg, M. C., and J. K. Horne (2009), Turbulence, acoustic backscatter, and pelagic nekton in Monterey Bay, *J. Phys. Oceanogr.*, *39*, 1097–1114, doi:10.1175/2008JPO4033.1.

Huntley, M. E., and M. Zhou (2004), Influence of animals on turbulence in the sea, *Mar. Ecol. Prog. Ser.*, *273*, 65–79, doi:10.3354/meps273065.

Katija, K., and J. O. Dabiri (2009), A viscosity-enhanced mechanism for biogenic ocean mixing, *Nature*, *460*, 624–626, doi:10.1038/nature08207.

Kunze, E., J. F. Dower, I. Beveridge, R. Dewey, and K. P. Bartlett (2006), Observations of biologically generated turbulence in a coastal inlet, *Science*, *313*, 1768–1770, doi:10.1126/science.1129378.

Kunze, E., J. F. Dower, R. Dewey, and E. A. D'Asaro (2007), Mixing it up with krill, *Science*, *318*, 1239, doi:10.1126/science.318.5854.1239b.

Lighthill, J. (1975), *Mathematical Biofluiddynamics*, *Reg. Conf. Ser. Appl. Math.*, vol. 17, Soc. for Ind. and Appl. Math., Philadelphia, Pa.

Lorke, A., and W. N. Probst (2010), In situ measurements of turbulence in fish shoals, *Limnol. Oceanogr.*, *55*, 354–364.

Munk, W. H. (1966), Abyssal recipes, *Deep Sea Res.*, *13*, 707–730.

Taylor, G. K., R. L. Nudds, and A. L. R. Thomas (2003), Flying and swimming animals cruise at a Strouhal number tuned for high power efficiency, *Nature*, *425*, 707–711, doi:10.1038/nature02000.

Thorpe, S. A. (2005), *The Turbulent Ocean*, Cambridge Univ. Press, Cambridge, U. K.

Turner, J. S. (1964), The flow into an expanding spherical vortex, *J. Fluid Mech.*, *18*, 195–208, doi:10.1017/S0022112064000155.

Visser, A. W. (2007), Biomixing of the oceans?, *Science*, *316*, 838–839, doi:10.1126/science.1141272.

White, B., and H. M. Nepf (2003), Scalar transport in random cylinder arrays at moderate Reynolds number, *J. Fluid Mech.*, *487*, 43–79, doi:10.1017/S0022112003004579.

Wunsch, C., and R. Ferrari (2004), Vertical mixing, energy, and the general circulation of the ocean, *Annu. Rev. Fluid Mech.*, *36*, 281–314, doi:10.1146/annurev.fluid.36.050802.122121.

J. O. Dabiri, Graduate Aeronautical Laboratories and Bioengineering, California Institute of Technology, Pasadena, CA 91125, USA. (jodabiri@caltech.edu)